International Journal of Electrical and Computer Engineering (IJECE)
Vol. 12, No. 5, October 2022, pp. 4808~4819
ISSN: 2088-8708, DOI: 10.11591/ijece.v12i5.pp4808-4819

Multi-phase inverter-controlled induction machine at varied rotor parameters

Crescent Onyebuchi Omeje[1], Damian Benneth Nnadi[2], Stephen Ejiofor Oti[2]
[1]Department of Electrical and Electronic Engineering, University of Port Harcourt, Rivers State, Nigeria
[2]Department of Electrical Engineering, University of Nigeria, Nsukka Enugu State, Nigeria

Article Info

Article history:

Received Sep 21, 2020
Revised Jun 17, 2022
Accepted Jun 27, 2022

Keywords:

Electromagnetic torque
Multi-level converters
Pulse width modulations
Six phase induction machines
Six-phase diode clamped

ABSTRACT

This paper presents a step-wise modelling of a symmetrical six-phase induction machine driven by a six-phase diode clamped multi-level inverter at a varying rotor resistance and motor inertia. The machine drive process was considered in two stages. The first stage presents the dynamic behavior of the machine when a load torque of 0 Nm and 100 Nm is applied at a varied rotor external resistance value of (0.8 and 3.2) Ω with constant motor inertia. The second stage showcased the variations in the speed, electromagnetic torque and rotor current when motor inertia is varied at 0.5 Kg-m^2 and 1.5 Kg-m^2 with rotor resistance held constant. A six-phase five-level diode clamped converter phase displaced by sixty degrees with a modulation index of 0.8 was modeled to drive the poly-phase machine at a reduced %THD. All machine models were simulated in MATLAB 7.11. The simulation results showed that reduced oscillations in rotor current, motor speed and torque pulsations were achieved at a varied external rotor resistance and motor inertia.

Corresponding Author:

Crescent Onyebuchi Omeje
Department of Electrical and Electronic Engineering, University of Port Harcourt
Rivers State, Nigeria
Email: crescent.omeje@uniport.edu.ng

1. INTRODUCTION

Induction machines are widely used in various areas and a vast range of energy conversion processes. Its applications can be found in low-power domestic devices to large industrial drives applications. These industrial applications may include ship propulsion, traction applications and electric vehicles operations [1]. At present, induction generators are particularly used in small and isolated power plants based on wind turbines or hydroelectric generators [2]–[4]. However, the power electronics developments, in conjunction with control theories, have spurred researchers to conduct substantial work on emergent applications relevant to asynchronous machines. Amongst the new emergent challenges, multiphase induction machines are considered the most promising solution for renewable energy applications [5]. Multiphase drives possess some advantageous features as compared to the conventional three-phase drives which include reduction in the amplitude of torque pulsation, better fault tolerance, higher efficiency, lower current ripple or reduction in the rotor harmonic current and the ease to split certain magnitude of power into multiple phases to reduce the power stress per phase [6], [7]. This power splitting enhances the proper use of the devices of less rating in case of moderate power application process [7]. The multiphase induction machine used in electric vehicles was studied in [8]. Though, no emphasis was made on the adjustable speed drives using a multilevel multiphase power converter source. Matrix converter as reported in [9] was used to drive a six-phase induction motor. This report though exhaustive did not highlight the comparative advantage of applying a higher-order multilevel converter in regulating the speed and torque of the machine at a varied rotor resistance and inertia. A work presented in [10], only considered the transient analysis model of induction motor with winding faults without recourse to the rotor current corrective measures with an injected rotor resistance. Renukadevi and Rajambal [11] developed a generalized model of multiphase induction motor with symmetrical winding displacement operation but the emphasis on the power converter control was not detailed. The use of a multiphase induction machine was proposed in [12], while the control of a five-phase induction motor using space vector modulation was discussed in [13]. These reviewed papers considered the high-performance back-stepping control strategy. Similarly, Mandal [14] considered the induction motor as an RL load having an improved power factor achieved by inserting a variable capacitor through a bridge converter which is adjusted for a unity value. These technical reports considered the steady-state characteristic behavior of the machine with a phase limitation of three. Therefore, no consideration of the speed and torque pulsation when operated with a higher-level power electronic converter at a varied load was discussed. This paper, in consideration of the above-reviewed journals, presents a complete dynamic model of a six-phase squirrel cage induction machine controlled by a six-phase multilevel diode clamped converter which is phase displaced by 60°. The carrier-based sinusoidal pulse width modulation was applied in the generation of the firing or gating signals of the converter switches at a switching frequency of 5 kHz. The choice of this frequency was to attenuate the effect of lower-order harmonics infiltrating into the machine. The developed model simulated in MATLAB/Simulink environment showed the characteristics performance of the machine under varied rotor resistance and motor inertia with a load torque of 0 Nm and 100 Nm.

2. METHOD: MODELLING OF THE SIX-PHASE SQUIRREL CAGE INDUCTION MACHINE

To develop the DQ model of the induction machine, some standard conditions were considered which include ensuring that the air gap between the windings was made uniform with the windings sinusoidally distributed around the air gap. The core loss and the magnetic saturation of the core were all neglected. The friction and windage losses in the system were also neglected to ensure the ideal condition of operation [15]. Since the stator winding was separated into two identical three-phase winding sets as shown in Figures 1 and 2, the usual Park's transformation can be applied to each three-phase set separately. Adopting the usual simplification, the voltage equations of the machine without rotor external resistance were represented by (1) to (6) in a synchronously rotating reference frame [16]. To enhance the reduction in high starting current of the machine due to the high slip value during starting period, an externally applied resistance is injected into the rotor terminal as shown in Figure 2. Thus, the rotor voltage equation under this condition changes to (7) to (8):

$$V_{qs1} = r_s i_{qs1} + p\lambda_{qs1} + \omega\lambda_{ds1} \tag{1}$$

$$V_{ds1} = r_s i_{ds1} + p\lambda_{ds1} - \omega\lambda_{qs1} \tag{2}$$

$$V_{qs2} = r_s i_{qs2} + p\lambda_{qs2} + \omega\lambda_{ds2} \tag{3}$$

$$V_{ds2} = r_s i_{ds2} + p\lambda_{ds2} - \omega\lambda_{qs2} \tag{4}$$

$$V'_{qr} = 0 = r'_r i'_{qr} + p\lambda'_{qr} + (\omega - \omega_r)\lambda'_{dr} \tag{5}$$

$$V'_{dr} = 0 = r'_r i'_{dr} + p\lambda'_{dr} - (\omega - \omega_r)\lambda'_{qr} \tag{6}$$

where $\rho = \frac{\mathrm{d}}{\mathrm{dt}}$.

$$V'_{qr} = 0 = (r'_r + r'_{ext})i'_{qr} + p\lambda'_{qr} + (\omega - \omega_r)\lambda'_{dr} \tag{7}$$

$$V'_{dr} = 0 = (r'_r + r'_{ext})i'_{dr} + p\lambda'_{dr} + (\omega - \omega_r)\lambda'_{qr} \tag{8}$$

The flux linkage equations were derived from Figures 1 and 2 with the actual equations presented in (9) to (14).

$$\lambda_{qs1} = L_{ls} i_{qs1} + L_{lm}(i_{qs1} + i_{qs2}) + L_m(i_{qs1} + i_{qs2} + i'_{qr}) \tag{9}$$

$$\lambda_{ds1} = L_{ls}i_{ds1} + L_{lm}(i_{ds1} + i_{ds2}) + L_m(i_{ds1} + i_{ds2} + i'_{dr}) \tag{10}$$

$$\lambda_{qs2} = L_{ls}i_{qs2} + L_{lm}\left(i_{qs1} + i_{qs2}\right) + L_m\left(i_{qs1} + i_{qs2} + i'_{qr}\right) \tag{11}$$

$$\lambda_{ds2} = L_{ls}i_{ds2} + L_{lm}(i_{ds1} + i_{ds2}) + L_m(i_{ds1} + i_{ds2} + i'_{dr}) \tag{12}$$

$$\lambda'_{qr} = L'_{lr}i'_{qr} + L_m\left(i_{qs1} + i_{qs2} + i'_{qr}\right) \tag{13}$$

$$\lambda'_{dr} = L'_{lr}i'_{dr} + L_m(i_{ds1} + i_{ds2} + i'_{dr}) \tag{14}$$

For ease in computer simulation, (1) to (14) were solved and arranged in state space and also represented in matrix form in (15) and (16).

$$\begin{bmatrix} A_{11}A_{12}A_{13}A_{14}A_{15}A_{16} \\ A_{21}A_{22}A_{23}A_{24}A_{25}A_{26} \\ A_{31}A_{32}A_{33}A_{34}A_{35}A_{36} \\ A_{41}A_{42}A_{43}A_{44}A_{45}A_{46} \\ A_{51}A_{52}A_{53}A_{54}A_{55}A_{56} \\ A_{61}A_{62}A_{63}A_{64}A_{65}A_{66} \end{bmatrix} \times \begin{bmatrix} \frac{di_{\mathrm{qs1}}}{dt} \\ \frac{di_{\mathrm{ds1}}}{dt} \\ \frac{di_{\mathrm{qs2}}}{dt} \\ \frac{di_{\mathrm{ds2}}}{dt} \\ \frac{di'_{\mathrm{qr}}}{dt} \\ \frac{di'_{\mathrm{dr}}}{dt} \end{bmatrix} = \begin{bmatrix} \mathrm{F}_{11} \\ \mathrm{F}_{22} \\ \mathrm{F}_{33} \\ \mathrm{F}_{44} \\ \mathrm{F}_{55} \\ \mathrm{F}_{66} \end{bmatrix} \tag{15}$$

$$\begin{bmatrix} \frac{di_{\mathrm{qs1}}}{dt} \\ \frac{di_{\mathrm{ds1}}}{dt} \\ \frac{di_{\mathrm{qs2}}}{dt} \\ \frac{di_{\mathrm{ds2}}}{dt} \\ \frac{di'_{\mathrm{qr}}}{dt} \\ \frac{di'_{\mathrm{dr}}}{dt} \end{bmatrix} = \begin{bmatrix} A_{11}A_{12}A_{13}A_{14}A_{15}A_{16} \\ A_{21}A_{22}A_{23}A_{24}A_{25}A_{26} \\ A_{31}A_{32}A_{33}A_{34}A_{35}A_{36} \\ A_{41}A_{42}A_{43}A_{44}A_{45}A_{46} \\ A_{51}A_{52}A_{53}A_{54}A_{55}A_{56} \\ A_{61}A_{62}A_{63}A_{64}A_{65}A_{66} \end{bmatrix}^{-1} \begin{bmatrix} \mathrm{F}_{11} \\ \mathrm{F}_{22} \\ \mathrm{F}_{33} \\ \mathrm{F}_{44} \\ \mathrm{F}_{55} \\ \mathrm{F}_{66} \end{bmatrix} \tag{16}$$

where: $A_{11} = L_{Ls} + L_{\mathrm{Lm}} + L_m$, $A_{12} = \mathrm{L_{Lm}} + L_{\mathrm{m}}$, $A_{13} = A_{14} = 0$, $A_{15} = \mathrm{L}_m$, $A_{16} = 0$, $A_{21} = A_{22} = 0$, $A_{23} = \mathrm{L_{Ls} + L_{Lm} + L_m}$, $A_{24} = \mathrm{L_{Lm} + L_m}$, $A_{25} = 0$, $A_{26} = \mathrm{L_m}$, $A_{31} = \mathrm{L_{Lm} + L_m}$, $A_{32} = \mathrm{L_{Ls} + L_{Lm} + L_m}$, $A_{33} = A_{34} = 0$, $A_{35} = \mathrm{L_m}$, $A_{36} = 0$, $A_{41} = 0$, $A_{42} = 0$, $A_{43} = \mathrm{L_{Lm} + L_m}$, $A_{44} = \mathrm{L_{Ls} + L_{Lm} + L_m}$, $A_{45} = 0$, $A_{46} = \mathrm{L_m}$, $A_{51} = A_{52} = \mathrm{L_m}$, $A_{53} = A_{54} = 0$, $A_{55} = \mathrm{L'_{Lr} + L_m}$, $A_{56} = 0$, $A_{61} = A_{62} = 0$, $A_{63} = \mathrm{L_m}$, $A_{64} = \mathrm{L_{Lm} + L_m}$, $A_{65} = 0$, $A_{66} = \mathrm{L'_{L_r} + L_m}$.

Similarly,

$\mathrm{F}_{11} = V_{qs1} - r_s i_{qs1} - \omega i_{ds1}(L_{Ls} + L_{\mathrm{Lm}} + L_m) - \omega i_{ds2}(L_{\mathrm{Lm}} + L_m) - \omega\, i'_{dr}L_m$,
$\mathrm{F}_{22} = V_{ds1} - r_s i_{ds1} + \omega i_{qs1}(L_{Ls} + L_{\mathrm{Lm}} + L_m) + \omega i_{q2}(L_{\mathrm{Lm}} + L_m) + \omega\, i'_{qr}L_m$,
$\mathrm{F}_{33} = V_{qs2} - r_s i_{qs2} - \omega i_{ds2}(L_{Ls} + L_{\mathrm{Lm}} + L_m) - \omega i_{ds1}(L_{\mathrm{Lm}} + L_m) - \omega\, i'_{dr}L_m$,
$\mathrm{F}_{44} = V_{ds2} - r_s i_{ds2} + \omega i_{qs2}(L_{Ls} + L_{\mathrm{Lm}} + L_m) + \omega i_{q1}(L_{\mathrm{Lm}} + L_m) + \omega\, i'_{qr}L_m$,
$\mathrm{F}_{55} = V'_{qr} - r'_r i'_{qr} - (\omega - \omega_r)i_{ds1}L_m - (\omega - \omega_r)i_{ds2}L_m - (\omega - \omega_r)i_{qs1}L_m - (\omega - \omega_r)\, i'_{dr}(L'_{Lr} + L_m)$,
$\mathrm{F}_{66} = V'_{dr} - r'_r i'_{dr} + (\omega - \omega_r)i_{qs1}L_m + (\omega - \omega_r)i_{qs2}L_m + (\omega - \omega_r)i_{ds1}L_m + (\omega - \omega_r)\, i'_{qr}(L'_{Lr} + L_m)$,

The electromagnetic torque in terms of flux linkage and current was presented in (17).

$$T_e = \left(\frac{3}{2}\right)\left(\frac{P}{2}\right)\left(\frac{L_m}{L'_{lr}}\right)\left[\psi'_{\mathrm{dr}}\left(i_{qs1} + i_{qs2}\right) - \psi'_{\mathrm{qr}}(i_{ds1} + i_{ds2})\right] \tag{17}$$

The rotor speed equation in terms of torque was represented in (18).

$$\omega_r = \frac{1}{J_r}\int (T_e - T_L)dt \quad (18)$$

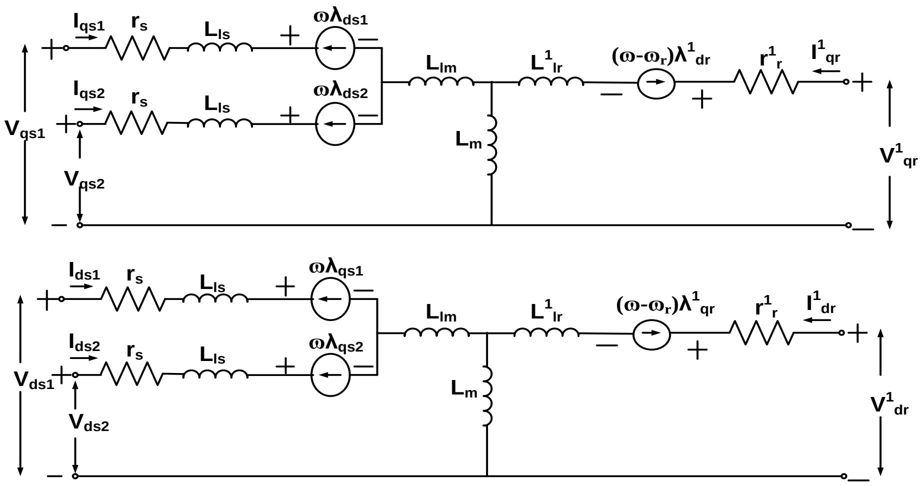

Figure 1. Per phase equivalent circuits of six-phase induction motor without external rotor resistance

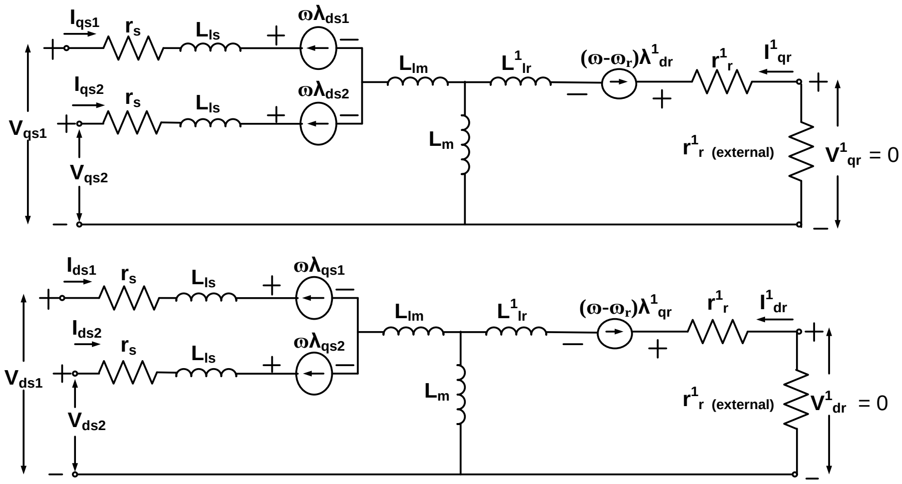

Figure 2. Per phase equivalent circuits of six phase induction motor with external rotor resistance

J_r is moment of inertia in Kgm^2, T_e is electromagnetic torque in Nm. ω_r is motor speed in radian per Sec. It is necessary to note that the concept of the multilevel converter was conceived with a three-level inverter by Baker [17], and Nabae *et al* [18]. Meynard and Foch in mid-1990 introduced a flying capacitor multi-level converters (FCC) inverter which is considered as another modification of multilevel inverter topology [19]. The basis of this inverter was the usage of capacitors as the source of supply to the inverter. The switching states in FCC inverter are similar to the NPC inverter. A multilevel converter, as reported in [20], has many attractive features including generation of output voltage with low harmonic distortions, production of smaller common-mode voltage that reduces the stress in the bearings of AC machines and operation at both fundamental switching frequency and high carrier frequency pulse width modulation. A multilevel converter application involving higher power may require multiphase systems to reduce the stress encountered on the switching devices. Generally, an increased number of switching devices increases the number of voltage levels whereas, in the multiphase converter, the number of phases of the converter in addition to the voltage level is increased [21]. The reports presented in [22]–[24] showed the possibilities of designing a machine with more than three phases and the increasing investigation on the modulation control of multiphase multilevel inverters. These reports though limited to five-phase was able to show the significance of the multiphase converter in the speed control of induction motor. Recently, conventional three-level five-phase inverters are employed for a five-phase, single motor drive [25], and five-phase dual motor drives [26]. It is observed that a large number of space vectors are generated due to the highly complex power circuit topology of the dual three-level inverters. The developed PWM schemes for three-level, five-phase inverters pose real-time implementation challenges due to the limited capability of the signal processors. The proposed six-phase multilevel diode clamped converter for this research paper is presented in Figure 3. This is a modification of the basic three-phase five-level diode clamped converter topology reported in reference [27]. Conventionally, a multiphase multilevel converter is always phase displaced by an angle theta represented by (19).

$$\theta = \frac{360}{N} \tag{19}$$

The PWM modulation techniques applied in this work for inverter simulations are referenced in [28]–[30].

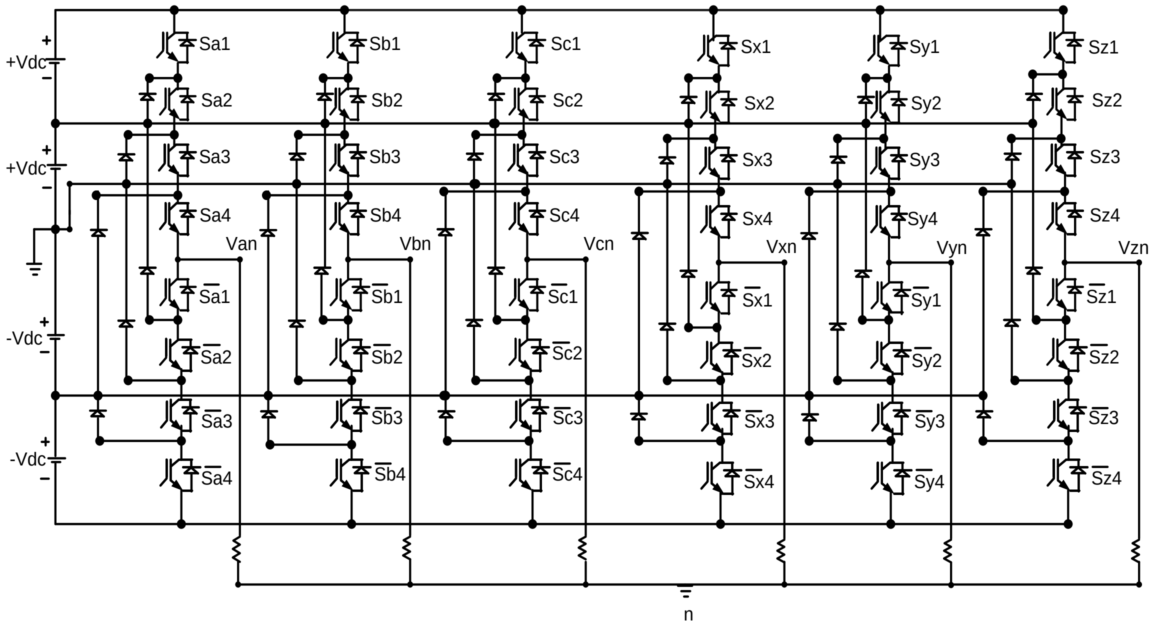

Figure 3. Equivalent circuit diagram of six phase multilevel diode clamped converter

3. RESULTS AND DISCUSSION

Simulation of a six-phase multi-level converter-controlled six-phase induction machine with a rotor injected external resistance at a varying load torque was carried out in MATLAB/Simulink. The waveforms of the electromagnetic torque, motor speed and rotor current which correspond to the changes in the applied load torque at varied rotor resistance and inertia are presented in Figures 4 to 14. In Figure 4, it is shown that the dq-axes stator current at a rotor resistance value of 3.2 Ω attains a steady-state at 0.25second as against 0.75 second achieved with 0.8 Ω rotor resistance with reduced oscillation. Similarly, in Figure 5, the dq-axes rotor current attains steady states at different simulation period of 0.23 second and 1.05 second for a rotor resistance value of 3.2 Ω. More so, with a rotor resistance value of 0.8 Ω, steady-state is attained at 0.805 second and 1.1 second with a pronounced oscillation. In Figure 6, it is shown that the overshoot, settling time and rise time are reduced when the rotor resistance is set to 3.2 Ω. At a simulation period of 1.0 second with an applied load torque of 100 Nm, a change in speed is achieved for the rotor resistance values of 0.8 Ω and 3.2 Ω. In Figure 7, the transient response in the electromechanical torque is high with 0.8 Ω rotor resistance. Though a rise in the value of the electromechanical torque is observed at 1.0 second due to an applied load torque of 100 Nm, the rate of torque pulsation is reduced as the rotor resistance is increased to 3.2 Ω. In Figure 8, a plot of torque against speed showed that the curl shape tends to diminish with 3.2 Ω. This indicates that the steady-state is achieved at a faster rate with 3.2 Ω than when 0.8 Ω is applied. Therefore, when J=0.5 Kgm^2 dq-axes stator current attains a steady-state condition at 0.5 second and also 1.0 second when the moment of inertia (J) is increased to 1.5 Kgm^2. In Figure 9, when the inertia J=1.5 Kgm^2 the transient period of oscillation for the dq-axes rotor current is increased to 1.0 second before attaining steady-state condition. Also, when J=0.5 Kgm^2, the transient period is reduced and a steady-state condition is attained at a shorter period of 0.5 second. In Figure 10, it is observed that when J=0.5 Kgm^2, torque pulsation is reduced. Steady-state for the electromechanical torque is attained at 0.55 second until a load torque of 100 Nm is applied at a simulation period of 1.0 second after which a rise in the electromechanical torque is obtained at 1.15 second. In like manner, when the moment of inertia is increased to J=1.5 Kgm^2, the rate of torque pulsation is increased. At a period of 1.0 second with the application of 100 Nm load torque, a fall in the electromechanical torque is observed which rises after a simulation period of 1.15 second and attains a steady state. In Figure 11, it is observed that the rise time and the rate of overshoot are achieved in a shorter period with J=0.5 Kgm^2. When a load of 100 Nm is applied, a drop in speed is obtained at 1.0 second which maintains a steady-state after 1.15 second. In Figure 12, a plot of torque against speed indicates that the rate of transient is more pronounced when J=1.5 Kgm^2 and less when J=0.5 Kgm^2. Figures 13 and 14 represent the stepped waveforms of the six-phase multi-level converter voltage with the corresponding values of total harmonic distortion. It is shown in these figures that the output voltage waveforms have the same amplitude with a successive phase displacement of 60° and a close-range in %THD. The phase and line voltages for the six-phase output are depicted in Figure 15.

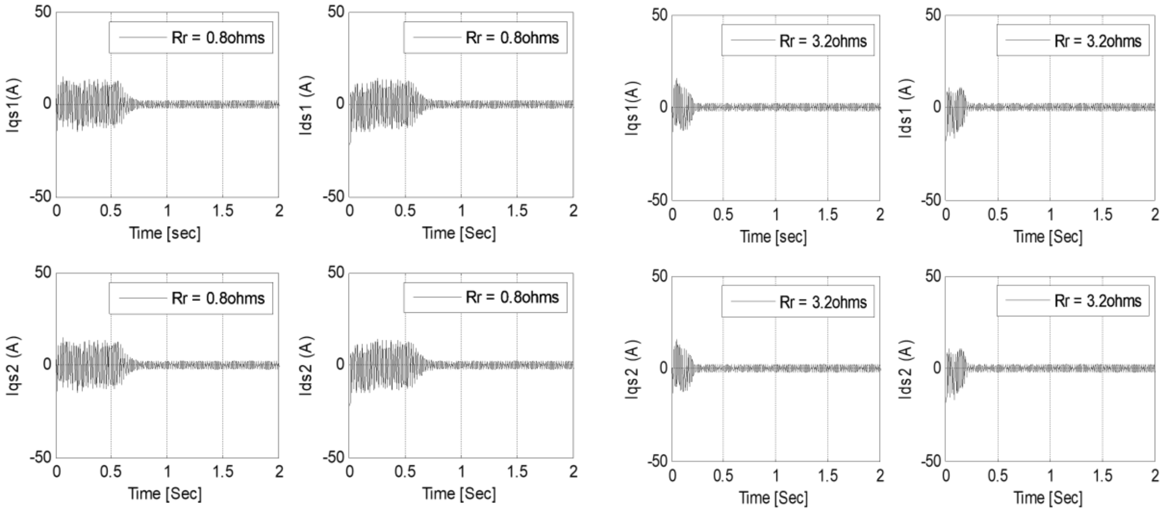

Figure 4. A plot of dq-axes stator current at resistance values of 0.8 Ω and 3.2 Ω

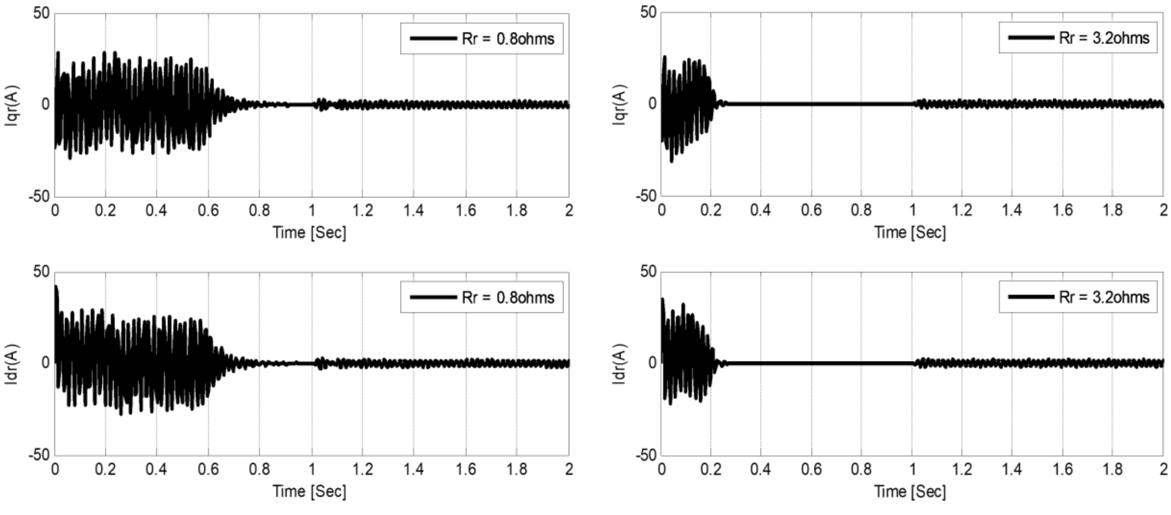

Figure 5. A plot of dq-axes rotor current at resistance values of 0.8 Ω and 3.2 Ω

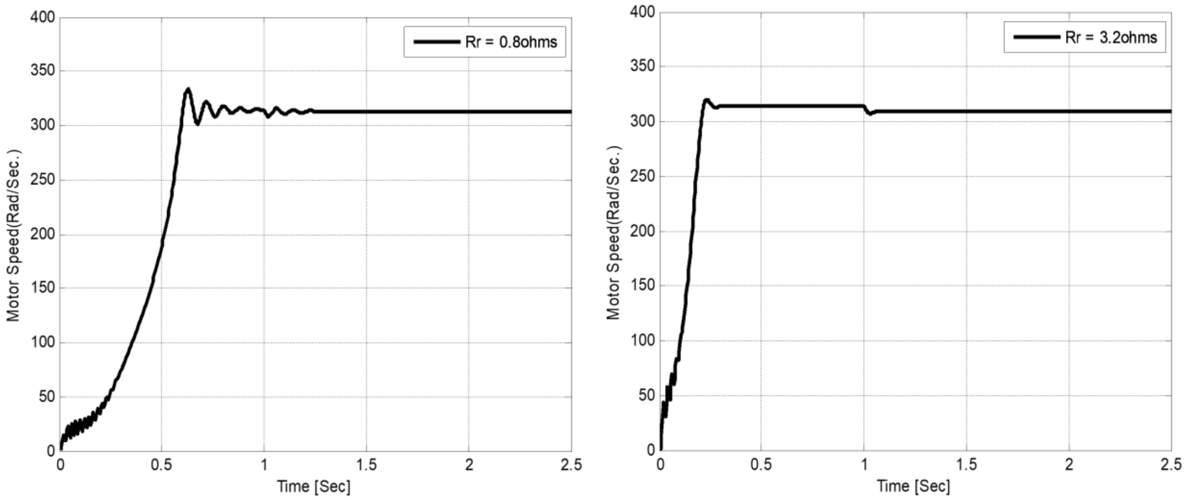

Figure 6. A plot of motor speed at resistance values of 0.8 Ω and 3.2 Ω

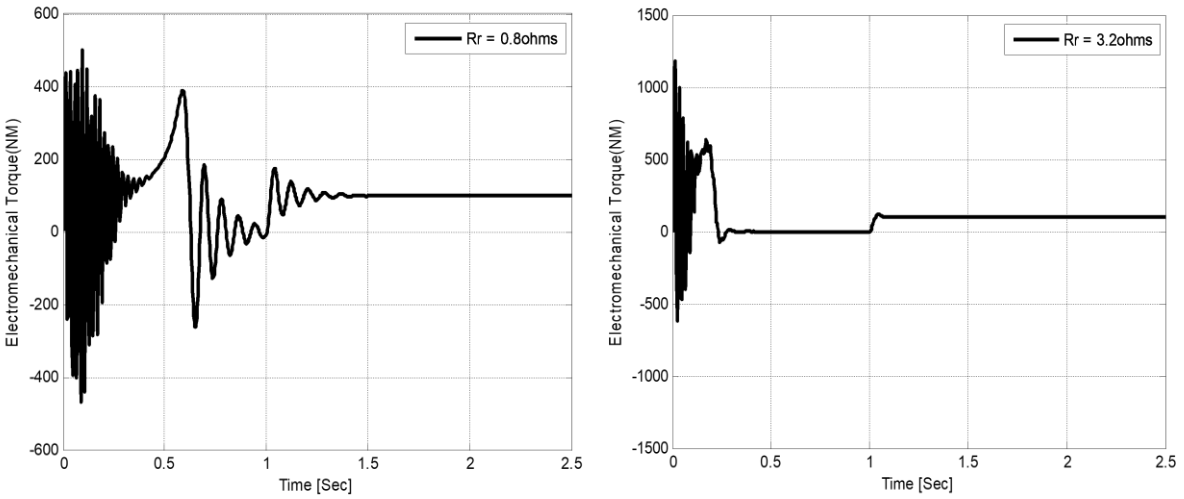

Figure 7. A plot of electromechanical torque at resistance values of 0.8 Ω and 3.2 Ω

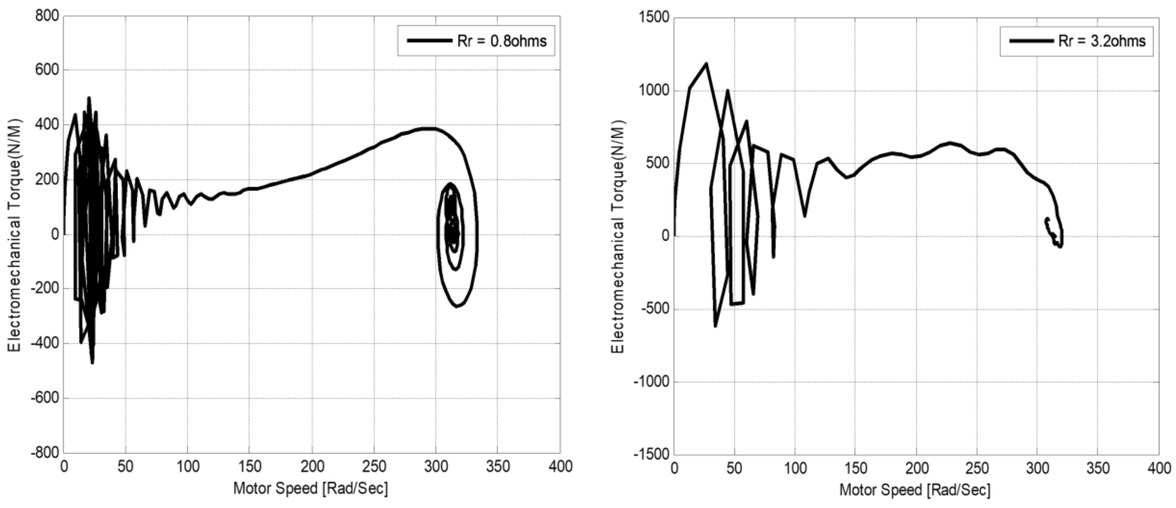

Figure 8. A plot of Tem (Nm) against ωr (Rad/Sec) at resistance values of 0.8 Ω and 3.2 Ω

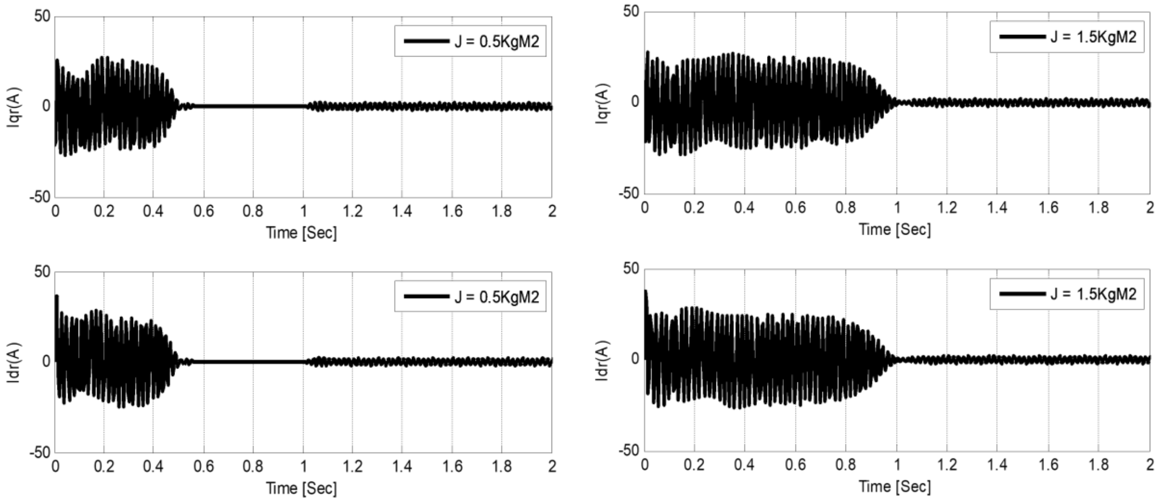

Figure 9. A plot of dq-axes rotor current at moment of inertia J=0.5 KgM^2 and 1.5 KgM^2

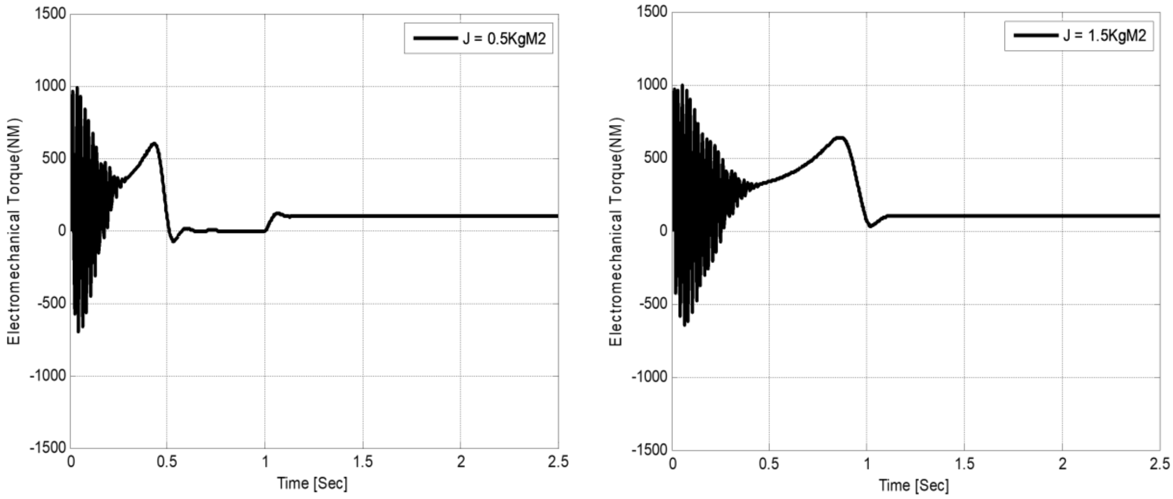

Figure 10. A plot of electromechanical torque at moment of inertia J=0.5 KgM^2 and 1.5 KgM^2

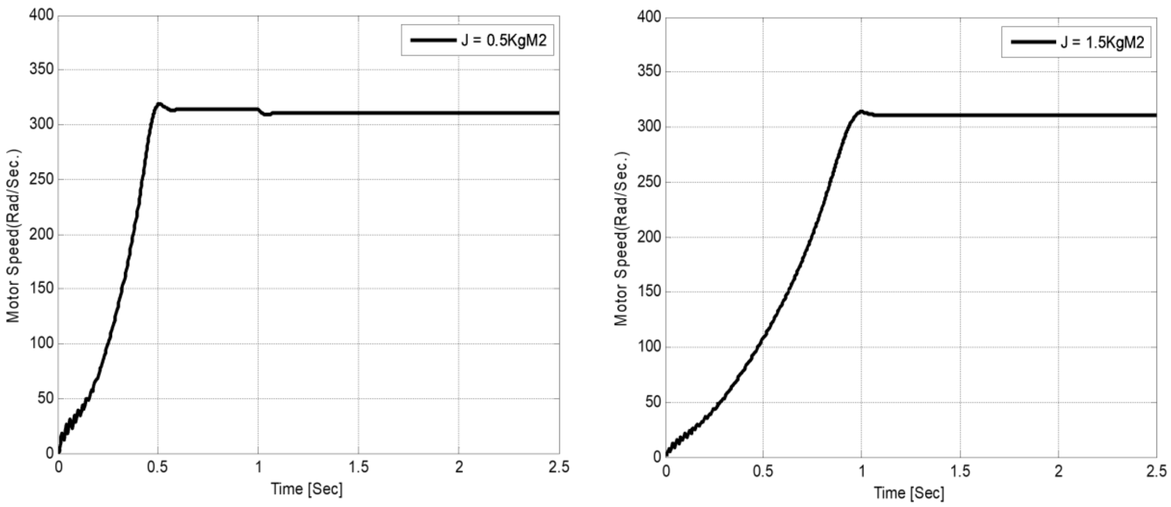

Figure 11. A plot of motor speed at moment of inertia J=0.5 KgM^2 and 1.5 KgM^2

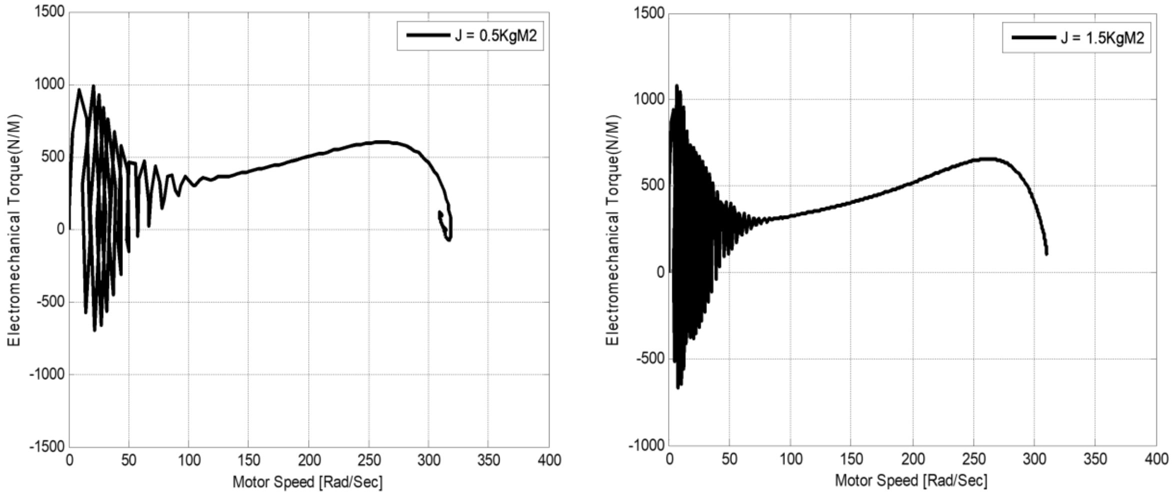

Figure 12. Electromechanical torque against speed at moment of inertia J=0.5 KgM^2 and 1.5 KgM^2

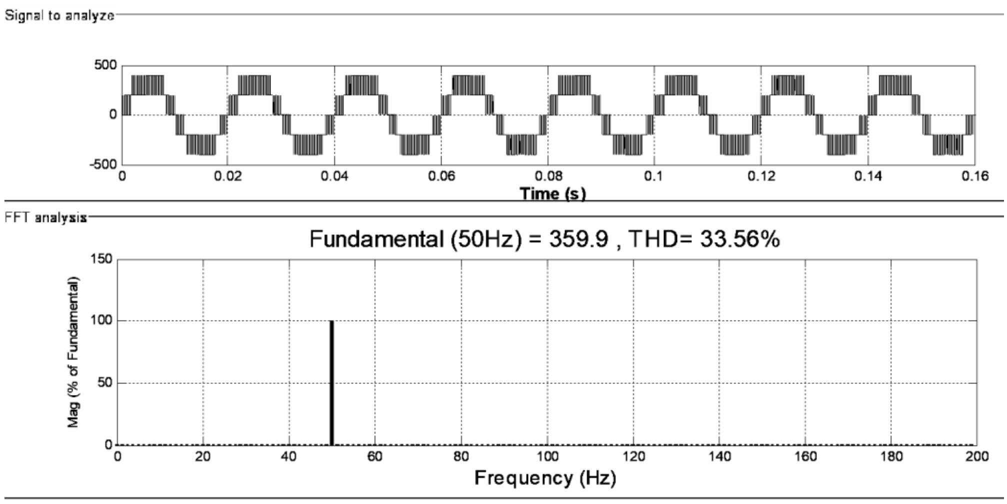

Figure 13. A plot of phase A voltage with %THD

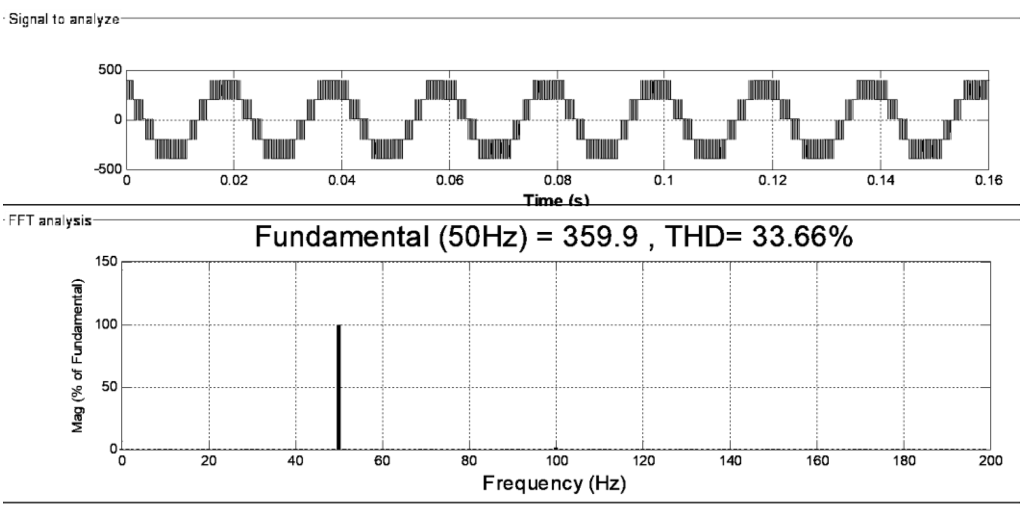

Figure 14. A plot of phase B voltage with %THD

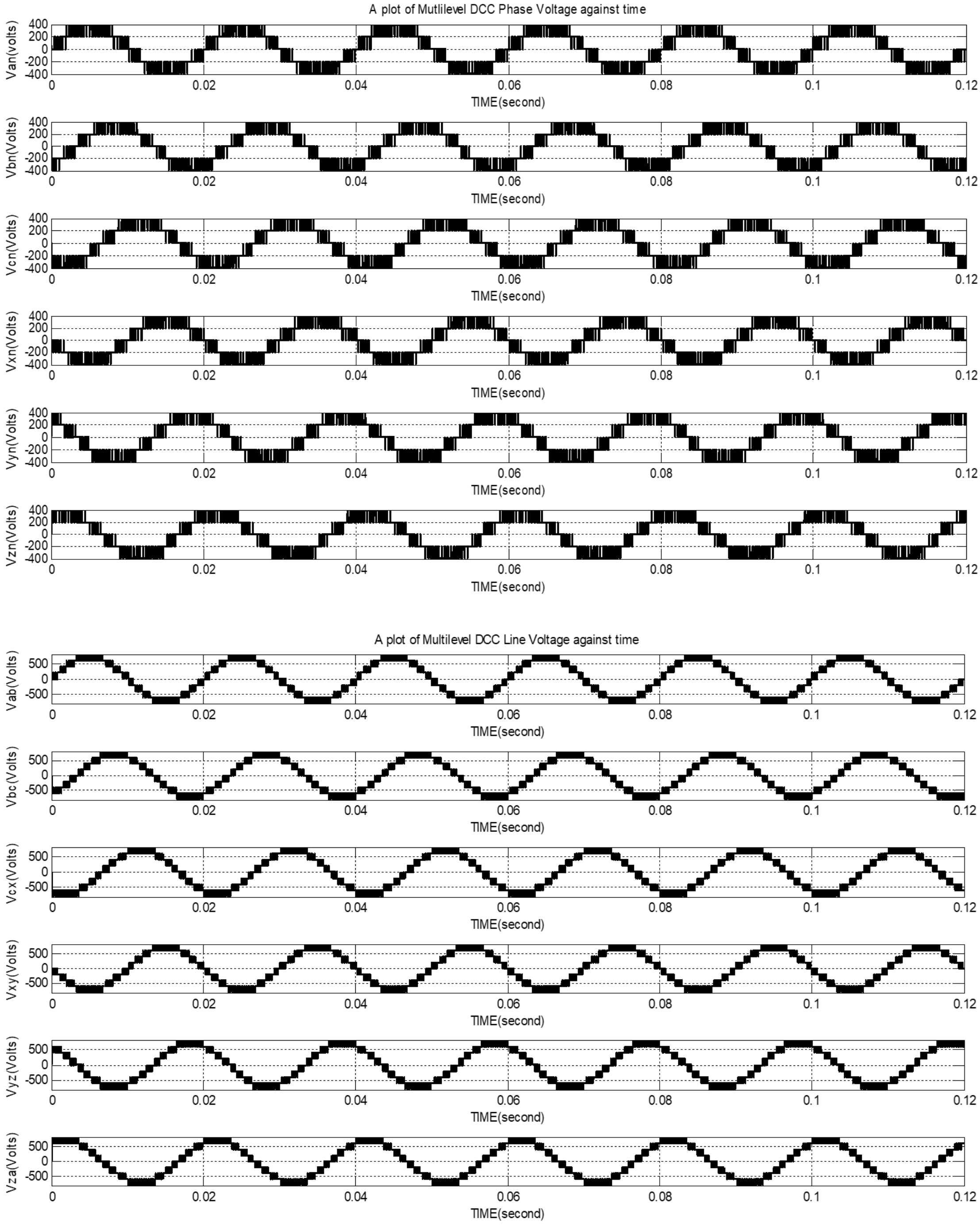

Figure 15. A plot of the phase and line-line voltages for the six-phase FCC

4. CONCLUSION

The simulation results portrayed the characteristics of a polyphase squirrel cage induction motor driven by a multi-level diode clamped converter. The dynamic performances of the machine under an applied load torque of 0 to 100 Nm were analyzed. At no load (0 Nm), the motor runs at a speed of 320 radian/second which is above the synchronous speed value of 314.2 radian per second for a two-pole machine as shown in Figure 6. When loaded at 100 Nm, the machine speed reduced from 320 radian per second to 310.1 radian per second which is below the synchronous speed also shown in Figures 11 and 12. A reduction in the amplitude of torque pulsation and the transient response was also observed on varying the rotor resistance and motor inertia. The flexibility in the adjustable motor drive performance was made possible with the 60° phase displaced six-phase multilevel diode clamped converter supply. This multilevel converter ensured that variable speed control is obtained from the adjustable frequency switching pattern of the pulse-width modulated inverter at a modulation index of 0.8. Hence, the complete dynamic model of a six-phase squirrel cage induction machine controlled by a six-phase multilevel diode clamped converter which is phase displaced by 60° can be recommended for a practical validation in the future work for industrial use due to its operational efficiency.

REFERENCES

[1] A. Kadaba, S. Suo, G. Y. Sizov, C.-C. Yeh, A. Sayed-Ahmed, and N. A. O. Demerdash, "Design and modeling of a reversible 3-phase to 6-phase induction motor for improved survivability," in *2011 IEEE Power and Energy Society General Meeting*, Jul. 2011, pp. 1–5, doi: 10.1109/PES.2011.6039812.

[2] G. K. Singh, K. B. Yadav, and R. P. Saini, "Analysis of a saturated multi-phase (six-phase) self-excited induction generator," *International Journal of Emerging Electric Power Systems*, vol. 7, no. 2, pp. 461–466, Sep. 2006, doi: 10.2202/1553-779X.1234.

[3] G. Aroquiadassou, H. Henao, and G.-A. Capolino, "Experimental analysis of the dq0 stator current component spectra of a 42V fault-tolerant six-phase induction machine drive with opened stator phases," in *2007 IEEE International Symposium on Diagnostics for Electric Machines, Power Electronics and Drives*, Sep. 2007, pp. 52–57, doi: 10.1109/DEMPED.2007.4393070.

[4] E. Levi, "Multiphase electric machines for variable-speed applications," *IEEE Transactions on Industrial Electronics*, vol. 55, no. 5, pp. 1893–1909, May 2008, doi: 10.1109/TIE.2008.918488.

[5] F. Bu, Y. Hu, W. Huang, S. Zhuang, and K. Shi, "Control strategy and dynamic performance of dual stator-winding induction generator variable frequency AC generating system with inductive and capacitive Loads," *IEEE Transactions on Power Electronics*, vol. 29, no. 4, pp. 1681–1692, Apr. 2014, doi: 10.1109/TPEL.2013.2265099.

[6] L. Parsa, "On advantages of multi-phase machines," in *31st Annual Conference of IEEE Industrial Electronics Society, 2005. IECON 2005.*, 2005, pp. 1574–1579, doi: 10.1109/IECON.2005.1569139.

[7] S. Islam, A. Iqbal, F. I. Bakhs, M. Saleh, and A. Kalam, "Stability analysis of a series-connected five-phase induction motor drive system using flux-linkage model," in *2013 IEEE 8th Conference on Industrial Electronics and Applications (ICIEA)*, Jun. 2013, pp. 445–450, doi: 10.1109/ICIEA.2013.6566410.

[8] A. Baltatanu and M.-L. Florea, "Multiphase machines used in electric vehicles propulsion," in *Proceedings of the International Conference on Electronics, Computers and Artificial Intelligence-ECAI-2013*, Jun. 2013, pp. 1–6, doi: 10.1109/ECAI.2013.6636204.

[9] H. Wang, R. Zhao, F. Cheng, and H. Yang, "Six-phase induction machine driven by the matrix converter," in *2011 International Conference on Electrical Machines and Systems*, Aug. 2011, pp. 1–5, doi: 10.1109/ICEMS.2011.6073641.

[10] V. Pahwa and K. S. Sandhu, "Transient analysis of three-phase induction machine using different reference frames," *ARPN Journal of Engineering and Applied Science*, vol. 14, no. 8, pp. 31–38, 2009.

[11] G. Renukadevi and K. Rajambal, "Generalized model of multi-phase induction motor drive using MATLAB/simulink," in *ISGT2011-India*, Dec. 2011, pp. 114–119, doi: 10.1109/ISET-India.2011.6145366.

[12] H. Ben Echikh, R. Trabelsi, M. F. Mirnouni, and F. M'sahli, "5-Phase AC induction motor rotor flux oriented control with space vector modulation technique," in *2013 International Conference on Electrical Engineering and Software Applications*, Mar. 2013, pp. 1–12, doi: 10.1109/ICEESA.2013.6578487.

[13] H. Echeikh, R. Trabelsi, M. F. Mimouni, A. Iqbal, and R. Alammari, "High performance backstepping control of a fivephase induction motor drive," in *2014 IEEE 23rd International Symposium on Industrial Electronics (ISIE)*, Jun. 2014, pp. 812–817, doi: 10.1109/ISIE.2014.6864716.

[14] S. Mandal, "Performance analysis of six-phase induction motor," *International Journal of Engineering Research and Technology*, vol. 4, pp. 589–593, 2015.

[15] R. Rinkeviciene, B. Kundrotas, and S. Lisauskas, "Model of controlled six phase induction motor," *International Journal of Electrical, Computer, Energetic, Electronic and Communication Engineering*, vol. 7, no. 1, pp. 56–61, 2013.

[16] C. M. Ong, *Dynamic simulation of electric machinery using MATLAB/Simulink*. New Jersey: New Jersey: Academic Press, 1998.

[17] R. H. Baker, "Bridge converter circuit," U.S. Patent 4270163, 1981.

[18] A. Nabae, I. Takahashi, and H. Akagi, "A new neutral-point-clamped PWM inverter," *IEEE Transactions on Industry Applications*, vol. IA-17, no. 5, pp. 518–523, Sep. 1981, doi: 10.1109/TIA.1981.4503992.

[19] C. Omeje, "A general review and performance evaluation of multi-level converters for efficient power generation and applications," *Nigerian Journal of Technology*, vol. 35, no. 1, pp. 174–189, Dec. 2015, doi: 10.4314/njt.v35i1.25.

[20] C. Odeh, "Fundamentals of a multi-phase, neutral-point clamped multilevel inverter," *Nigerian Journal of Technology*, vol. 33, no. 3, p. 375, Jul. 2014, doi: 10.4314/njt.v33i3.16.

[21] J. W. Kelly, E. G. Strangas, and J. M. Miller, "Multiphase space vector pulse width modulation," *IEEE Transactions on Energy Conversion*, vol. 18, no. 2, pp. 259–264, Jun. 2003, doi: 10.1109/TEC.2003.811725.

[22] H. A. Toliyat, "Analysis and simulation of five-phase variable-speed induction motor drives under asymmetrical connections," *IEEE Transactions on Power Electronics*, vol. 13, no. 4, pp. 748–756, Jul. 1998, doi: 10.1109/63.704150.

[23] A. Iqbal and E. Levi, "Space vector PWM techniques for sinusoidal output voltage generation with a five-phase voltage source inverter," *Electric Power Components and Systems*, vol. 34, no. 2, pp. 119–140, Feb. 2006, doi: 10.1080/15325000500244427.

[24] B. Kundrotas, S. Lisauskas, R. Rinkeviciene, and A. Smilgevicius, "Six phase induction machine drive and dynamic characteristics investigation," in *International Conference on Electrical and Control Technologies*, 2011, pp. 218–221.

[25] L. Gao and J. E. Fletcher, "A space vector switching strategy for three-level five-phase inverter drives," *IEEE Transactions on Industrial Electronics*, vol. 57, no. 7, pp. 2332–2343, Jul. 2010, doi: 10.1109/TIE.2009.2033087.

[26] N. R. Abjadi, J. Soltani, J. Askari, and A. Markadeh, "Three-level five-phase space vector PWM inverter for a two five-phase series connected induction machine drive," *Energy and Power Engineering*, vol. 02, no. 01, pp. 10–17, 2010, doi: 10.4236/epe.2010.21003.

[27] B. Wu, *High-power converter and AC drives*. New Jersey, USA: Wiley, 2006.

[28] G. Carrara, S. Gardella, M. Marchesoni, R. Salutari, and G. Sciutto, "A new multilevel PWM method: a theoretical analysis," *IEEE Transactions on Power Electronics*, vol. 7, no. 3, pp. 497–505, Jul. 1992, doi: 10.1109/63.145137.

[29] D. Moha and S. B. Kurub, "A comparative analysis of multi-carriers SPWM Control strategies using fifteen level cascaded h-bridge multi-level inverter," *International Journal of Computer Application*, vol. 41, no. 21, pp. 7–11, 2012.

[30] C. O. Omeje, D. B. Nnadi, and I. C. Odeh, "Analysis of harmonic injection to the modulation of multilevel diode clamped converter in a normal and over modulation mode," *Nigerian Journal of Technology*, vol. 32, no. 1, pp. 67–80, 2013.

BIOGRAPHIES OF AUTHORS

Crescent Onyebuchi Omeje received his Bachelor's degree in Electrical Engineering, in 2004 from University of Nigeria, Nsukka. He also obtained his Masters of Engineering (M.Eng) and Doctor of Philosophy (Ph.D) in 2011 and 2019 respectively in Electrical Engineering, from the same University. He is a Member of Nigeria Society of Engineers (MNSE), a registered member Council for the regulation of Engineering in Nigeria (COREN), a member of the Institute of Electrical/Electronic Engineering (IEEE) and a full-time lecturer in the Department of Electrical/Electronic Engineering, University of Port Harcourt, Rivers State, Nigeria. He has published widely in local and international journals. His research interests include but not limited to power electronics, new energy conversion system, multilevel inverter applications, Electric motor drives and control, Power systems modeling. Email: crescent.omeje@uniport.edu.ng.

Damian Benneth Nnadi is presently a lecturer and a Professor in the Department of Electrical Engineering UNN. His university education was at Enugu State University of Science and Technology (ESUT), Enugu from 1993 to 1999, there, he obtained a B.Eng. (Electrical/Electronic). He got his M.Eng. degree also from Enugu State University of Science and Technology (ESUT) from 2002 to 2004. He has also obtained a Ph. D. in Power Electronics option from Electrical Engineering, University of Nigeria, Nsukka in 2014. He is a member of the Nigerian Society of Engineers (NSE). He is the current financial secretary of Nsukka Chapter of the Nigerian Institute of Electrical and Electronic Engineering (NIEEE) and he is also a registered member of the Council for the Regulation of Engineering in Nigeria (COREN). He is a member of the Industrial/Power Electronics and New/Renewable Energy Research Group, Power system/High Voltage Research Group. He can be contacted at email: damian.nnadi@unn.edu.ng.

Stephen Ejiofor Oti lives at the Garden of Edem in Umuchagwu Edem-Ani in Nsukka Local Government Area of Enugu state of Nigeria. He received a B.Eng. (Electrical Engineering), an M.Eng. (Electrical Power Devices) and a Ph.D. (Electrical Power Devices) degree, all of the University of Nigeria in 1998, 2006 and 2014 respectively. He joined the Electrical Engineering Department, UNN as a Principal Technical Officer and was later in 2007 converted to the lecturing cadre in the same department. He is a member of the Nigerian Society of Engineers (NSE). He is the current membership secretary of Nsukka Chapter of the Nigerian Institute of Electrical and Electronic Engineering (NIEEE) and he is also a registered member of the Council for the Regulation of Engineering in Nigeria (COREN). He has several research articles published in local and international journals. His research areas include Machine modeling, Thermal modeling, Power and Energy systems modeling and Simulations. He can be contacted at: stephen.oti@unn.edu.ng.